

Coherent superposition of M-states in a single rovibrational level of H₂ by Stark-induced adiabatic Raman passage

Nandini Mukherjee, Wenrui Dong, and Richard N. Zare

Citation: *The Journal of Chemical Physics* **140**, 074201 (2014); doi: 10.1063/1.4865131

View online: <http://dx.doi.org/10.1063/1.4865131>

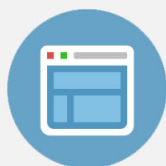
View Table of Contents: <http://scitation.aip.org/content/aip/journal/jcp/140/7?ver=pdfcov>

Published by the [AIP Publishing](#)



Re-register for Table of Content Alerts

Create a profile.



Sign up today!



Coherent superposition of M -states in a single rovibrational level of H_2 by Stark-induced adiabatic Raman passage

Nandini Mukherjee, Wenrui Dong, and Richard N. Zare

Department of Chemistry, Stanford University, Stanford, California 94305-5080, USA

(Received 18 December 2013; accepted 27 January 2014; published online 18 February 2014)

We prepare an ensemble of isolated rovibrationally excited ($v = 1, J = 2$) H_2 molecules in a phase-locked superposition of magnetic sublevels M using Stark-induced adiabatic Raman passage with linearly polarized single-mode pump (at 532 nm, ~ 6 ns pulse duration, 200 mJ/pulse) and Stokes (699 nm, ~ 4 ns pulse duration, 20 mJ/pulse) laser excitation. A biaxial superposition state, given by $|\psi(t)\rangle = 1/\sqrt{2}[|v = 1, J = 2, M = -2\rangle - |v = 1, J = 2, M = +2\rangle]$, is prepared with linearly but cross-polarized pump and Stokes laser pulses copropagating along the quantization z -axis. The degree of phase coherence is measured by using the O(2) line of the H_2 E,F-X (0,1) band via $2 + 1$ resonance enhanced multiphoton ionization (REMPI) at 210.8 nm by recording interference fringes in the REMPI signal in a time-of-flight mass spectrometer as the direction of the UV laser polarization is rotated using a half-wave plate. Nearly 60% population transfer from H_2 ($v = 0, J = 0$) ground state to the superposition state in H_2 ($v = 1, J = 2$) is measured from the depletion of the Q(0) line of the E,F-X (0,0) band as the Stokes frequency is tuned across the ($v = 0, J = 0$) \rightarrow ($v = 1, J = 2$) Raman resonance. © 2014 AIP Publishing LLC. [<http://dx.doi.org/10.1063/1.4865131>]

INTRODUCTION

To compare a benchmark atom-diatom scattering experiment ($H + H_2$) with theory without the statistical averaging over a thermal distribution of initial states, there is much interest in preparing the target molecule (H_2) in a well-defined rovibrational M -eigenstate, $|vJM\rangle$.¹ For this purpose we report the preparation of H_2 molecules in a molecular beam in a coherent superposition of eigenstates for a particular rovibrational level, ($v = 1, J = 2$). A coherent superposition of input channels might allow us to observe the geometrical phase effect which is otherwise hidden by the thermal averaging over uncorrelated initial (v, J, M) states.² We believe that this procedure is general and opens possibilities for investigations of phase-locked reaction dynamics.

Although considerable effort has been spent in the past to prepare a rovibrational (v, J, M) eigenstate, to our knowledge a stereodynamical reaction has never been possible with either a single or a superposition of M sublevel of H_2 . This is because, in the collision-free ambience of a molecular beam, traditional off-resonant Raman pumping has been unsuccessful in preparing a rovibrational quantum state for a sizable population of H_2 .^{3,4} Likewise, the resonantly enhanced Raman adiabatic techniques such as the stimulated Raman adiabatic passage (STIRAP)^{5,6} and, Stark chirped Raman adiabatic passage (SCRAP),⁷⁻⁹ are not suitable to prepare quantum states of H_2 because of the wide energy gap between the ground state and accessible excited electronic states. To prepare hydrogen molecules using these resonant techniques, the requirement of appropriate VUV laser sources and ionization loss poses a practical challenge. To overcome these limitations and to transfer significant population to a rovibrational (v, J, M) eigenstate of the H_2 molecule we use a coherent optical technique based on Stark-induced adiabatic Raman passage (SARP),¹⁰⁻¹² which does not require an intermedi-

ate resonance. Using SARP, we demonstrated nearly complete population transfer from an initial H_2 ($v = 0, J = 0$) ground state to a vibrationally excited H_2 ($v = 1, J = 0$) state within the ground electronic surface.¹² This was achieved using off-resonant Raman pumping with partially overlapping nanosecond visible (532 nm) pump and Stokes (683 nm) laser pulses. The detailed mechanism of SARP has been described in Refs. 10–12. In this work we demonstrate that by combining different polarizations of the pump and Stokes fields SARP can also prepare a coherent superposition of M eigenstates within the rovibrational ($v > 0, J$) energy eigenstate $E_{v,J}$:

$$\psi_{v,J} = \exp(-iE_{v,J}t/\hbar) \sum_M C_M |v, J, M\rangle, \quad (1)$$

where the coefficients C_M are time-independent complex numbers. $|C_M|^2$ is proportional to the M -sublevel population whereas $C_M^* C_{M'} (M \neq M')$ are the off-diagonal density matrix elements representing M -sublevel coherences. As opposed to wave-packets, the above superposition is a stationary state evolving with a single frequency $E_{v,J}/\hbar$; as a result, it will not be dispersed in time, which is most desirable for a collision experiment. When the target is prepared in a superposition state given in Eq. (1), the state-resolved differential scattering cross section will contain cross terms (interference terms) given by

$$\frac{d\sigma(v', J', \theta, \varphi)}{d\Omega} = \left(\frac{d\sigma}{d\Omega} \right)_{M\text{-averaged}} + \sum_{M \neq M'} C_M^* C_{M'} Q_{MM'}. \quad (2)$$

The first term in the right hand side of Eq. (2) is the M -sublevel-averaged collision cross section for a polarized H_2 target and is weighted by the population proportional to $|C_M|^2$

of various M -sublevels.

$$\left(\frac{d\sigma}{d\Omega}\right)_{M\text{-Averaged}} = \sum_M |C_M|^2 \sum_{M'} |q(v', J', M' \leftarrow v, J, M | \hat{r})|^2. \quad (3)$$

Here the $q(v', J', M' \leftarrow v, J, M | \hat{r})$ are the state-to-state reaction amplitudes in the direction $\hat{r}(\theta, \phi)$ defined relative to a coordinate system in the center-of-mass frame. Note that no phase information of the state-to-state reaction amplitudes q can be determined from the M -averaged collision cross section given by Eq. (3). The second term in the right hand side of Eq. (2), is proportional to $C_M^* C_{M'}$, and gives rise to interference in the collision probability. The maxima and minima of this interference are determined by the phases of the coefficients C_M . In other words, by controlling their relative phase, we can expect to control the outcome of a collision experiment.

The phase information of the state-to-state reaction amplitude is contained in $Q_{MM'}$,

$$Q_{MM'} = \sum_{M''} q^*(M'', v', J' \leftarrow v, J, M) \times q(M'', v', J' \leftarrow v, J, M'). \quad (4)$$

Thus, by preparing reacting molecules in a well-defined superposition of M -eigenstates, it is possible to extract both the phase and magnitude of the reaction amplitudes q . In essence, the M -sublevel superposition behaves much like a multi-slit interferometer where the number of slits, i.e., the number of M sublevels, and their separations (i.e., the relative phase) can be varied experimentally, thereby, directing the course of a collision. We note that similar coherent control of molecular scattering using M -state superposition has been suggested earlier by Brumer, Shapiro and co-workers.¹³⁻¹⁵ This work demonstrates how SARP prepares a significant portion of the ground state H_2 ($v = 0, J = 0$) population in a phase-locked superposition of $M = \pm 2$ states of H_2 ($v = 1, J = 2$) within the ground electronic state. The phase coherence of the superposition is measured by using interference of $2 + 1$ resonance enhanced multiphoton ionization channels.

PREPARATION OF THE M -SUBLEVEL SUPERPOSITION

Figure 1(a) shows the S(0) scheme ($v = 0, J = 0$) \rightarrow ($v = 1, J = 2$) of Raman pumping using right (E^-) and left (E^+) circularly polarized pump and Stokes laser optical fields. For convenience of presentation, the target level is drawn vertically above the virtual intermediate level. Figure 1(a) refers to the coordinate system shown in Fig. 1(b), where the quantization z -axis is oriented along the propagation direction of the pump and Stokes laser pulses. The transverse optical fields lie in the x - y plane. The circularly polarized field components (E^\pm) are derived from the linearly polarized pump and Stokes laser fields shown in Fig. 1(b). The subscripts P and S refer to the pump and Stokes laser pulses. The right and left circularly polarized pump and Stokes optical fields coherently tie the M sublevels of the ($v = 1, J = 2$)

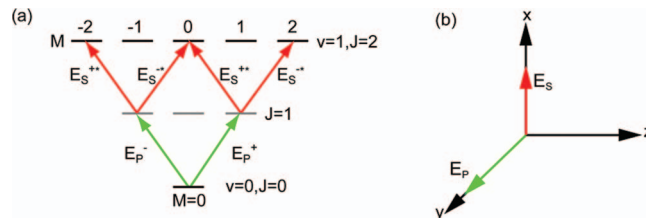


FIG. 1. (a) SARP excitation scheme to prepare an M -sublevel superposition using left and right circularly polarized pump and Stokes laser pulses. (b) Molecular center-of-mass coordinate system with the z -axis oriented along the laser propagation direction. The left and right circularly polarized components of the optical fields (Fig. 1(a)) are derived from the linearly polarized transverse pump and Stokes waves as described in the text.

level. For the special case of linearly polarized pump optical field along the y -direction and the Stokes optical field along the x -direction as shown in Fig. 1(b) we can write

$$E_P^+ = i \frac{E_P}{\sqrt{2}}, E_P^- = i \frac{E_P}{\sqrt{2}}, \quad (5)$$

$$E_S^+ = -\frac{E_S}{\sqrt{2}}, E_S^- = \frac{E_S}{\sqrt{2}}.$$

With the circularly polarized pump and Stokes optical field components of Eq. (5), the Raman excitation channels connecting the ground ($v = 0, J = 0, M = 0$) with the excited ($v = 1, J = 2, M = 0$) state interfere destructively transferring no population to the ($v = 1, J = 2, M = 0$) level,

$$E_P^- E_S^{*+} + E_P^+ E_S^{*-} = 0. \quad (6)$$

In the absence of population transfer to the ($v = 1, J = 2, M = 0$) level, SARP creates the following biaxial superposition within the H_2 ($v = 1, J = 2$) level:

$$|\psi(t)\rangle = 1/\sqrt{2} [|v = 1, J = 2, M = -2\rangle - |v = 1, J = 2, M = +2\rangle]. \quad (7)$$

In the following we describe an experiment to measure the population transfer and phase coherence of the superposition state in Eq. (7) prepared by SARP with cross-polarized pump and Stokes laser fields. When the linearly polarized pump and Stokes laser fields are parallel, for example, oriented along the x -axis, SARP prepares the following M -entangled superposition state:

$$|\psi(t)\rangle = \sqrt{\frac{3}{8}} |v = 1, J = 2, M = -2\rangle - \frac{1}{2} |v = 1, J = 2, M = 0\rangle + \sqrt{\frac{3}{8}} |v = 1, J = 2, M = +2\rangle. \quad (8)$$

For us, the state in Eq. (8) serves as the benchmark for characterizing the phase coherence of the prepared superposition state using the O(2) line of the H_2 E,F-X (0,1) band via the $2 + 1$ REMPI process.

DETECTION OF THE M -SUBLEVEL SUPERPOSITION

Detection of M -sublevel coherence requires measuring the interference ($C_M^* C_{M'}$) among the M -sublevel amplitudes. Experimentally, this is accomplished by using the interference of the resonance-enhanced multiphoton ionization chan-

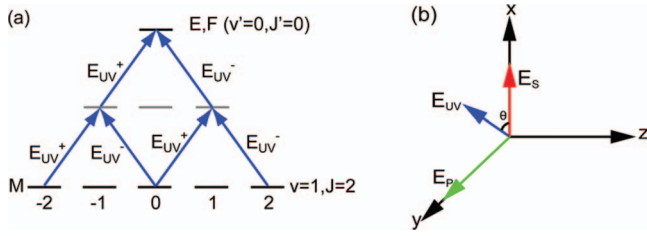


FIG. 2. (a) $2 + 1$ O(2) REMPI excitation scheme to detect M -sublevel coherence using polarized UV laser pulses. (b) Rotated polarization direction of UV laser optical field relative to the direction (x) of the Stokes laser field. All laser beams propagate parallel to the quantization z -axis. The left and right circular components of the UV laser polarization are derived from the linear polarization.

nels associated with the O(2) line of the $E, F^1\Sigma_g^+(v' = 0, J' = 0) - X^1\Sigma_g^+(v = 1, J = 2)$ transition. To illustrate this idea, we consider, for example, an arbitrary superposition state created by SARP following the excitation scheme described in Fig. 1(a):

$$\psi_{v=1, J=2} = C_-|M = -2\rangle + C_0|M = 0\rangle + C_+|M = +2\rangle. \quad (9)$$

Here $C_{\pm, 0}$ are the amplitudes of $M = 0, \pm 2$ sublevels of the H_2 ($v = 1, J = 2$) target level, where the quantization z -axis is the same as defined in Fig. 1(b). Figure 2(a) shows the O(2) ionization scheme from the M sublevels of the SARP prepared H_2 ($v = 1, J = 2$) level within the ground $X^1\Sigma_g^+$ electronic state via the two-photon resonant $H_2(v' = 0, J' = 0)$ level of the excited $E, F^1\Sigma_g^+$ electronic state. Figure 2(b) shows the orientation of the linearly polarized UV probe optical field relative to the pump and Stokes laser fields. E_{uv}^+ and E_{uv}^- are the left and right circular components making up the linearly polarized optical field of the UV light. We calculate the $2 + 1$ REMPI signal that results from the interference of different ionization channels from the expression

$$O(2) \propto \left| C_- E_{uv}^{+2} + \sqrt{\frac{2}{3}} C_0 E_{uv}^+ E_{uv}^- + C_+ E_{uv}^{-2} \right|^2. \quad (10)$$

For the linearly polarized UV probe field at an angle θ with respect to the x -axis (Fig. 2(b)) we have

$$E_{uv}^+ = -\frac{E_{uv}}{\sqrt{2}} e^{-i\theta} \quad \text{and} \quad E_{uv}^- = \frac{E_{uv}}{\sqrt{2}} e^{i\theta}. \quad (11)$$

Substituting the fields of Eq. (11) into Eq. (10), the $2 + 1$ REMPI signal can be expressed as a function of the angle θ of the UV laser polarization,

$$O(2) \propto \left| C_- e^{+2i\theta} - \sqrt{\frac{2}{3}} C_0 + C_+ e^{-2i\theta} \right|^2. \quad (12)$$

The $2 + 1$ REMPI signal in Eq. (12) generates interference fringes as a function of the UV polarization angle θ . The visibility (contrast) of an interference fringe is directly related to the phase coherence of the constituent M sublevels. In the following we describe an experiment to measure the phase coherence using the fringe visibility of the ionization signal.

EXPERIMENTAL METHOD

The detail experimental arrangement of SARP is described in Refs. 11 and 12. In summary, a supersonic beam of H_2 molecules inside a vacuum chamber is transversely intercepted by a delayed sequence of nanosecond single-mode pump (fixed frequency 532 nm, ~ 6 ns) and Stokes (variable frequency near 699 nm, ~ 4 ns) laser pulses. A time delay of ~ 4 – 5 ns between the pump and Stokes laser pulse is established using an optical delay line in the path of the pump laser beam. The pump and Stokes laser polarizations are set by using Glan-Thompson polarizers (extinction ratio $\sim 100\,000$) in their respective beam path before combing them on a beam-splitter. The relative polarization of the pump and Stokes laser fields are adjusted using a half-wave retarder in the path of the pump laser beam. In spite of the high extinction ratio of the Glan-polarizers, the final laser beams are slightly elliptical owing to (a) finite curvature of the phase front of the pulsed laser beams and (b) birefringence of the optics. To reach the threshold fluence required by SARP, the pump and Stokes laser beams are focused on the molecular beam axis using a 40-cm focal length lens. The estimated fluence at the focus is nearly 17 J/mm^2 for the pump and 1.5 J/mm^2 for the Stokes. A weaker UV probe laser beam (energy ~ 0.5 mJ) is counterpropagated and is focused on the molecular beam axis slightly downstream relative to the pump and Stokes laser beams using a 20-cm focal length lens. The UV laser is tuned to the peak of $(2 + 1)$ REMPI transition from the ground ($v = 0, J = 0$) or excited ($v = 1, J = 2$) rovibrational levels. The REMPI-generated ions are collected by using a time-of-flight mass spectrometer with its flight tube oriented perpendicular to the molecular and laser beam propagation directions. To avoid AC Stark shift of the REMPI signal, the UV laser pulses are delayed by 20 ns with respect to the pump and Stokes laser pulses. Population transfer to the target state is measured by the depletion of the Q(0) branch of $E, F^1\Sigma_g^+(v' = 0, J' = 0) - X^1\Sigma_g^+(v = 0, J = 0)$ REMPI signal as a function of the Stokes laser frequency ω_S . Here ω_S is tuned across the field-free Raman resonance defined by $(\omega_P - \omega_S) - \omega_{10} = 0$, where $\omega_{P,S}$ are the pump and Stokes laser frequencies and ω_{10} is the field-free Raman resonance frequency for $(v = 0, J = 0) \rightarrow (v = 1, J = 2)$ transition.

From the depletion of ground H_2 ($v = 0, J = 0$) level REMPI signal we measure nearly 60% population transfer to H_2 ($v = 1, J = 2$) level prepared by SARP with cross-polarized or parallel pump and Stokes laser optical fields. Figure 3 shows a recording of the Q(0) REMPI signal as a function of the Stokes laser frequency in THz for SARP pumping of H_2 ($v = 0, J = 0$) \rightarrow H_2 ($v = 1, J = 2$) with parallel polarization of the pump and Stokes laser pulses. Each experimental data point represents an average over 20 laser pulses. Compared to our previous experiments where SARP achieved nearly complete population transfer from H_2 ($v = 0, J = 0$) to H_2 ($v = 1, J = 0$), the present transition has much stronger AC Stark sweeping rate, which in turn requires a higher Stokes fluence. This explains why we observed 60% population transfer instead of complete transfer.

Figure 3, however, does not tell us how the population in $v = 1, J = 2$ is distributed among the M sublevels, or the

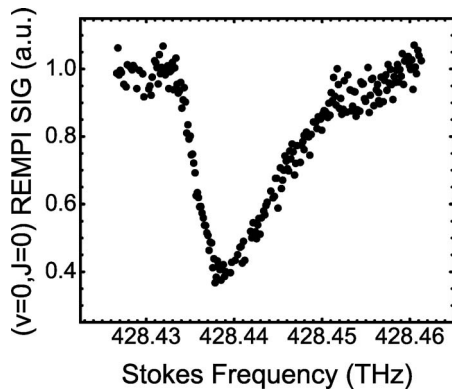


FIG. 3. Depletion of the Q(0) branch of $E, F^1\Sigma_g^+(v'=0, J'=0) - X^1\Sigma_g^+(v=0, J=0)$ REMPI signal as a function of Stokes laser frequency in THz. The depletion calibrates population transfer from the ground $H_2(v=0, J=0) \rightarrow H_2(v=1, J=2)$ level.

relative phase of the M -sublevel probability amplitudes. The relative amplitude of M sublevels can be measured using the interference fringe of the $2+1$ O(2) REMPI signal [Eq. (12)] as a function of the polarization angle of the UV laser field as described earlier. This measurement is accomplished by rotating the polarization direction of the linearly polarized UV probe laser (210.8 nm) electric field using a piezo-driven half-wave retarder with angular accuracy of $\pm 0.02^\circ$.

Figure 4(a) shows the experimental O(2) REMPI for the $H_2(v=1, J=2)$ level prepared by SARP with the parallel pump and Stokes lasers optical fields oriented along x as described in Eq. (8). O(2) REMPI is shown as a function of the polarization angle θ of the UV laser field defined with respect to the x -axis. The fringe contrast measures the phase coherence among the M -sublevels. Best fitting of the experimental fringe with Eq. (12) suggests $C_+ = C_-$, and $C_0/C_\pm \approx -1$ instead of the ratio ~ -0.82 as expected from Eq. (8). Figure 4(b) shows a 3D polar plot of the angular momentum polarization of the SARP prepared H_2 -state described by the second-order alignment parameters $A_0^{(2)} = 1/3$

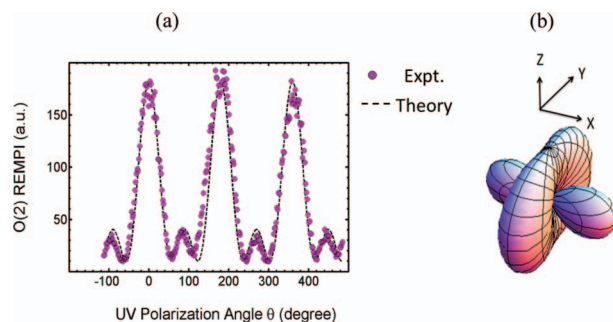


FIG. 4. (a) Experimental $E, F^1\Sigma_g^+(v'=0, J'=0) - X^1\Sigma_g^+(v=0, J=0)$ O(2) REMPI signal as a function of the UV probe laser polarization angle θ with respect to the direction (x) of the Stokes polarization. The $H_2(v=1, J=2)$ level in the ground $X^1\Sigma_g^+$ electronic state is prepared by the parallel polarizations of pump and Stokes laser fields (parallel SARP). Data are fitted using Eq. (12) with $C_0 = -0.6$, $C_\pm = +0.6$. (b) 3D polar plot of angular momentum polarization for the prepared state with second-order alignment parameters $A_0^{(2)} = 1/3$ and $A_\pm^{(2)} = -2/3$ calculated using the fitted values of amplitudes.

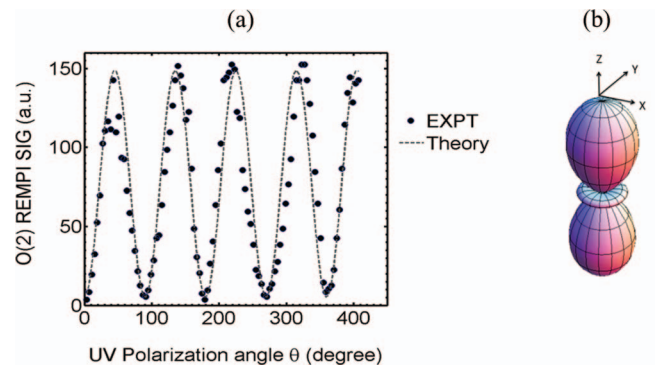


FIG. 5. (a) $E, F^1\Sigma_g^+(v'=0, J'=0) - X^1\Sigma_g^+(v=1, J=2)$ O(2) REMPI from $H_2(v=1, J=2)$ excited state prepared by SARP with perpendicular polarization of the pump and Stokes laser pulses. The REMPI signal is plotted against the polarization direction angle θ of the UV laser relative to the direction of the Stokes polarization (x). Data are fitted using Eq. (12) with $C_0 = 0$, $C_- = +1/\sqrt{2}$, $C_+ = -1/\sqrt{2}$. (b) 3D polar plot of the angular momentum polarization with the alignment parameters $A_0^{(2)} = 1$ and $A_\pm^{(2)} = 0$ calculated using the fitted values of the M -state amplitudes.

and $A_\pm^{(2)} = -2/3$. These alignment parameters are calculated using the best-fitted M -sublevel amplitudes¹⁶ which differ from the expected values $A_0^{(2)} = 0.5$ and $A_\pm^{(2)} = -0.612$ calculated using the amplitudes of Eq. (8). This discrepancy may have been caused by the rotation of the plane of polarization of the UV probe laser field because of the tight focusing with a 20-cm focal length lens. In this case a z -component of the probe field will be created to distort the expected interference.

Figure 5 shows the O(2) REMPI interference fringe for the target level $H_2(v=1, J=2)$ prepared by SARP using cross-polarized pump and Stokes lasers electric fields (perpendicular SARP) as described above in Fig. 1 and Eq. (7). In spite of the sharp fringe visibility which is the hallmark of coherence, fitting of the experimental data using Eq. (12) shows in Fig. 5(a) some discrepancy in the periodicity of the ion fringes. At this time, it is not clear why the experimentally measured points do not lie more closely about the theoretically predicted REMPI signal. Nuclear depolarization is ruled out because the $J=2$ rotational level of H_2 has zero nuclear spin. Also, the effect cannot be caused by a slight misalignment of the parallel and perpendicular polarization directions. In such cases the M -asymmetry of the prepared state will reduce the REMPI fringe contrast, but will not generate the observed discrepancy [see Eq. (12)]. The sharp fringe contrast suggests that we have achieved fairly pure alignment with nearly equal amplitudes in $M = \pm 2$ states, that is, $C_-/C_+ \approx -1$ and $C_0 \approx 0$ as expected from Eq. (7). As a further test, we examined the polarizations of the pump and Stokes laser pulses transmitted through the chamber and did not find significant rotation of their orthogonal state of polarization. We suspect that the discrepancy may have been an artifact caused by either a nonuniform motion of the rotation stage or a nonuniform coating of the half-wave plate at 211 nm, or both.

Figure 5(b) shows a 3D polar plot of the corresponding angular momentum polarization of the biaxial state calculated using the alignment parameters $A_0^{(2)} = 1$ and $A_\pm^{(2)} = 0$.

DISCUSSION

Our experiment demonstrates that SARP can create a large ensemble of isolated rovibrationally excited H_2 ($v = 1, J = 2$) molecules in a coherently coupled M -sublevel superposition using appropriate polarizations of the pump and Stokes laser optical fields. We determine the relative phase of entanglement by measuring interference of ionization channels associated with the $O(2)$ line of $(2 + 1)$ REMPI signal. These examples showed M -sublevel superposition with a fixed relative phase. Using a different scheme of SARP excitation, it is possible to vary the relative phase of a biaxial superposition as pictured by the excitation scheme of Fig. 6. For example, by using SARP with a linearly polarized pump pulse propagating along the z -direction and a Stokes pulse propagating along the y -direction it is possible to prepare the following superposition state (see Fig. 6):

$$|\psi(t)\rangle = 1/\sqrt{2}[|v = 1, J = 2, M = -1\rangle - e^{-i2\alpha} |v = 1, J = 2, M = +1\rangle]. \quad (13)$$

Note that SARP is able to prepare such a biaxial superposition state because the AC Stark shift is proportional to M^2 , that is, the energy of $M = \pm|M|$ states will be synchronously Stark-chirped by the laser intensity. Theory suggests that it is also possible to use elliptic polarization to coherently mix $M = 0$ and $M = \pm 2$ sublevels, even though the $M = 0$ sublevel has a different Stark shift. Such preparation is achieved by the Raman coupling among the M -sublevels of $J = 2$ with $\Delta M = \pm 2$. Using the excitation scheme of Fig. 6, the relative phase (2α) of the superposition can be continuously varied by rotating the direction of linearly polarized pump electric field in the x - y plane. Similar perpendicular propagation of the pump and Stokes lasers has been used by STIRAP to achieve M -sublevel superpositions.^{5,6} In essence such coher-

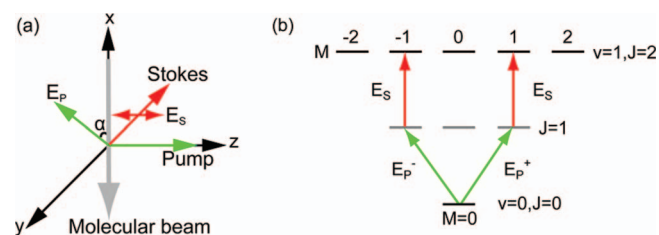


FIG. 6. Preparation of superposition states with variable relative phase. (a) Necessary pump and Stokes laser beam geometry to prepare the state in Eq. (13). (b) Three-level excitation scheme with the pump and Stokes polarizations of (a).

ent superposition is equivalent to a molecular interferometer for the incident flux of particles whose scattering will be determined by the phase of the scatterer. The present technique of preparing an M -sublevel superposition of molecules like H_2 finally opens the possibility to measure the phase of the reaction amplitude. We believe that such phase measurements will significantly advance our understanding of chemical reactions by connecting more closely theory and experiment at the quantum level.

ACKNOWLEDGMENTS

This work was supported by the U.S. Army Research Office under ARO Grant No. W911NF-13-1-0126 and a DURIP equipment Grant No. W911NF-11-1-0342.

We gratefully acknowledge the financial support from a subcontract with the Yale University Agreement No. C13J225+(J00210) for which the Army Research Office Grant No. W911NF-12-1-0476 is the prime sponsor. All authors were supported by the above.

- ¹R. N. Zare, *Annu. Rev. Phys. Chem.* **64**, 1 (2013); A. E. Pomerantz, F. Ausfelder, R. N. Zare, S. C. Althorpe, F. J. Aoiz, L. Bañares, and J. F. Castillo, *J. Chem. Phys.* **120**, 3244 (2004).
- ²J. C. Juanes-Marcos, S. C. Althorpe, and E. Wrede, *Science* **309**, 1227 (2005).
- ³P. Maroni, D. Papageorgopoulos, A. Ruf, R. D. Beck, and T. R. Rizzo, *Rev. Sci. Instrum.* **77**, 054103 (2006); N. C.-M. Bartlett, J. Jankunas, and R. N. Zare, *J. Chem. Phys.* **134**, 234310 (2011).
- ⁴N. Mukherjee and R. N. Zare, *J. Chem. Phys.* **135**, 184202 (2011).
- ⁵K. Bergman, H. Theuer, and B. W. Shore, *Rev. Mod. Phys.* **70**, 1003 (1998).
- ⁶Z. Kis, N. V. Vitanov, A. Karpati, C. Barthel, and K. Bergmann, *Phys. Rev. A* **72**, 033403 (2005).
- ⁷N. V. Vitanov, M. Fleischhauer, B. W. Shore, and K. Bergmann, *Adv. At., Mol., Opt. Phys.* **46**, 55 (2001).
- ⁸T. Ricketts, L. P. Yatsenko, S. Steuerwald, T. Halfmann, B. W. Shore, N. V. Vitanov, and K. Bergmann, *J. Chem. Phys.* **113**, 534 (2000).
- ⁹L. P. Yatsenko, N. V. Vitanov, B. W. Shore, T. Ricketts, and K. Bergmann, *Opt. Commun.* **204**, 413 (2002); M. Heinz, F. Vewinger, U. Schneider, L. P. Yatsenko, and K. Bergmann, *ibid.* **264**, 248 (2006).
- ¹⁰N. Mukherjee and R. N. Zare, *J. Chem. Phys.* **135**, 024201 (2011).
- ¹¹N. Mukherjee, W. Dong, J. A. Harrison, and R. N. Zare, *J. Chem. Phys.* **138**, 051101 (2013).
- ¹²W. Dong, N. Mukherjee, and R. N. Zare, *J. Chem. Phys.* **139**, 074204 (2013).
- ¹³M. Shapiro and P. Brumer, in *International Reviews in Physical Chemistry* (Taylor & Francis, London, 1994), Vol. 13, p. 187; *Phys. Rev. Lett.* **77**, 2574 (1996).
- ¹⁴P. Brumer and M. Shapiro, *Annu. Rev. Phys. Chem.* **43**, 257 (1992).
- ¹⁵C. A. Arango, M. Shapiro, and P. Brumer, *Phys. Rev. Lett.* **97**, 193202 (2006); *J. Chem. Phys.* **125**, 094315 (2006).
- ¹⁶A. J. Orr-Ewing and R. N. Zare, *Annu. Rev. Phys. Chem.* **45**, 315 (1994).